Kitaichi N, Shimizu T, Honda A, Abe R, Ohgami K, Shiratori K, Shimizu H, Ohno S.	Increase of macrophage migration inhibitory factor levels in lacrimal fluid of patients with severe atopic dermatitis.	Graefes Arch Clin Exp Ophthalmol	244	825-8	2006
Chi A, Valencia JC, Hu Z, Watabe H, Yamaguchi H, Mangini NJ, Huang H, Canfield VA, Cheng KC, Abe R, Yamagishi S, Shabanowitz J, Hearing VJ, Wu C, Appella E, Hunt DF.	Proteomics and Bioinformatics Characterization of the biogenesis and function of melanosomes.	J Proteome Res	5	3135-44	2006
Tanimura S, Arita K, Iwao F, Kasai M, Fujita Y, Kawasaki H, Abe R, Sawamura D, Kimura T, Shimizu H.	Two cases of folliculosebaceous cystic hamartoma.	Clin Exp Dermatol	31	68-70	2006
Murata J, Shimizu T, Tateishi Y, Abe R, Shimizu H.	Coexistence of systemic lupus erythematosus and porphyria cutanea tarda-a case successfully improved by avoidance of sun exposure-.	Int J Dermatol	45	435-7	2006

Yanagi T, Shimizu T, Ujiie H, Ito M, Abe R, Tsuji-Abe Y, Hige S, Shimizu H	Peginterferon alfa-2b for mycosis fungoides.	Arch Dermatol	142	649-651	2006
Natsuga K, Shimizu T, Abe R, Kodama K, Shimizu H.	Mycosis fungoides bullosa.	Arch Dermatol	142	793-5	2006
Osawa R, Abe R, Inokuma D, Yokota K, Ito H, Nabeshima M, Shimizu H.	Chain saw granuloma : reaction to the deep implanted chain saw fragment.	Arch Dermatol	142	1079-80	2006
Inoue A, Takahashi KA, Arai Y, Tonomura H, Sakao K, Saito M, Fujioka M, Fujiwara H, Tabata Y, Kubo T.	The therapeutic effects of basic fibroblast grwoth factor contained in gelatin hydrogel microspheres on experimental osteoarthritis in the rabbit knee.	Arth Rheum/ARC RES	54(1)	264-70	2006
Nagato H, Umebayashi H, Wako M, Tabata Y, Manabe M.	Collagen-PGA hybrid matrix with bFGF accelerated angiogenesis and granulation tissue formation in diabetic mice.	J Dermatol	33	670-5	2006
Nakae M, Kimura H, Naruse K, Horio N,	Effects of basic fobroblast growth factor	Diabetes	55	1470-7	2006

Ito Y, Mizubayashi R, Hamada Y, Nakashima E, Akiyama N, Kobayashi Y, Wtarai A, Kimura N, Horuguchi M, Tabata Y, Oisa Y, Nakamura J.	on experimental diabetic neuropathy in rats.				
Yamamoto M, Takahashi Y, Tabata Y.	Enhanced bone regeneration at a segmental bone defect by controlled release of bone morphogenetic protein-2 from a biodegradable hydrogel.	Tissue Eng	12(5)	1305-11	2006
Hiraoka Y, Yamashiro H, Yasuda K, Kimura Y, Inamoto T, Tabata Y.	In situ regeneration of adipose tissue in rat fat pad by combining a collagen scaffold with gelatin microspheres containing basic fibroblast growth factor.	Tissue Eng	12(6)	1475-87	2006
Takahashi S, Qin Chen, Ogushi T, Fujimura T, Kumagai J, Matsumoto S, Hijikata S, Tabata Y, Kitamura T.	Periurethral injection of sustained release basic fibroblast growth factor improves sphincteric contractility of the rat urethra	J Urology	176	819-23	2006

	denervated by botulinum-A toxin.				
Hirose K, Fujita M, Marui A, Arai Y, Sakaguchi H, Yuhong Huang, Shyamal Chandra BIR, Tabata Y, Komeda M.	Combined treatment of sustained-release basic fibroblast growth factor and sarpogrelate enhances collateral blood flow effectively in rabbit hindlimb ischemia.	Circ J	70	1190-4	2006
Hamada Y, Katoh S, Hibino N, Kosaka H, Hamada D, Yasui N, Ozeki M, Tabata Y.	Effects of monofilament nylon coated with basic fibroblast growth factor on endogenous intrasynovial flexor tendon healing.	J Hand Surg	31A	530-40	2006
Tazaki J, Akazawa T, Murata M, Yamamoto M, Tabata Y, YoshimotoR, Arisue M.	BMP-2 dose-response and rerease studies in functionally graded Hap.	Key Eng Mater	18	965-8	2006
Alejandro Soto-Gutierrez, Kobayashhi N, Jorge David Rivas-Carrillo, Nalu Navarro-Alvarez, Debaio Zhao, Okitsu T, Noguchi H, Hesham Basma, Tabata Y,	Reversal of mouse hepatic failure using an implanted liver-assist device containing ES cell-derived hepatocytes.	Nat Biotechnol	24	1412-9	2006

Yong Chen, Tanaka K, Narushima M, Miki A, Ueda T, Hee-Sook Jun, Tanaka N, Jane Lebkowski, Ji-Won Yoon, Ira J Fox.					
Iwai K, Nakagawa T, Endo T, Matsuoka Y, Kita T, T. S. Kim, Tabata Y, Ito J.	Cochlear protection by local IGF-1 application using biodegradable gel.	Laryngoscope	116 (4)	529-33	2006
Tanaka M, Tkayama A, Ito E, Sunami H, Yamamoto S, Shimomura M.	Effect of pore size of self-organized honeycomb-patterned polymer films on spreading, focal adhesion, proliferation, and function of endothelial cells	J nanosci Nanotechno	7	763-72	2007
Tanaka M, Nishikawa K, Okubo H, Kamachi H, Kawai T, Matsushita M, Todo S, Shimomura M.	Control of hepatocyte adhesion and function on self-organized honeycomb-patterned polymer film	Colloid Surface A	284-285	464-9	2006
Tsuruma A, Tanaka M, Yamamoto S, Fukushima N, Shimomura M.	Topographical control of neurites extension on stripe-patterned polymer films	Colloid Surface A	284-285	470-4	2006

Yamamoto S, Tanaka M, Sunami H, Arai K, Takayama A, Yamashita S, Morita Y, Shimomura M.	Relationship between adsorbed fibronectin and cell adhesion on a honeycomb-patterned Film	Surf Sci	600	3785-91	2006
Sunami H, Ito E, Tanaka M, Yamamoto S Shimomura M.	Effect of Honetcomb Films on protein Adhesion, Cell adhesion and proliferation	Colloid Surface A	284-285	548-51	2006
Yabu H, Hirai Y, Shimomura M.	Electroless Plating of Honeycomb and Pincushion Polymer Films Prepared by Self-Organization	Langmuir	22(23)	9760-4	2006
Okajima T, Tanaka M, Tsukiyama S, Kadowaki T, Yamamoto S, Shimomura M, Tokumoto H.	Stress relaxation of HepG2 cells measured by atmic force microscopy	Nanotechnology	18	1-5	2007
Uraki Y, Nemoto J, Otsuka H, Tamai Y, Sugiyama J, Kishimoto T, Ubukata M, Yabu H, Tanaka M, Shimomura M.	Honeycomb-Like Architecture Produced by Living Bacteria, Gluconacetobacter xylinus	Carbohyd Polym (in press)			
Chen YM, Tanaka M, Gong JP, Yasuda K, Yamamoto S, Shimomura M, Osada Y.	Platelet adhesion to endothelial cells cultured on various hydrogel scaffolds	Biomaterials	28	1752-60	2007

Higuchi T, Yabu H, Shimomura M.	Simple Preparation of Hemispherical Polystyrene Nanoparticles	Colloid Surface A	284-285	250-3	2006
Yabu H, Kojima M, Tsubouchi M, Onoue S, Sugitani M, Shimomura M.	Fabrication of Photo Cross-Linked Honeycomb-patterned Films	Colloid Surface A	284-285	254-6	2006
Yabu H, Inoue K, Shimomura M.	Multiple-periodic Structures of Self-organized Honeycomb-patterned Films and Polymer Nanoparticles Hybrids	Colloid Surface A	284-285	301-4	2006
Matsushita S, Shimomura M.	Light-propagation patterns in freestanding two-dimensional colloidal crystals	Colloid Surface A	284-285	315-9	2006
Tamaki K, Yabu H, Isoshima T, Hara M, Shimomura M.	Fabrication of luminescent polymeric nanoparticles doped with a lanthanide complex by self-organization process	Colloid Surface A	284-285	355-8	2006
Ohzono T, Shimomura M.	Simple fabrication of ring-like microwrinkle patterns	Colloid Surface A	284-285	505-8	2006

IV. 研究成果の刊行物・別刷

Possible Involvement of Exon 31 Alternative Splicing in Phenotype and Severity of Epidermolysis Bullosa Caused by Mutations in *PLEC1*

Journal of Investigative Dermatology advance online publication, 1 February 2007; doi:10.1038/sj.jid.5700707

TO THE EDITOR

Epidermolysis bullosa constitutes a group of phenotypically diverse genodermatoses which manifest with blistering and erosions of the skin and mucous membranes (Fine *et al.*, 2000). Recent advances in epidermolysis bullosa research have allowed the identification of mutations in 10 different genes, which account for the clinical heterogeneity in epidermolysis bullosa (Pulkkinen and Uitto, 1999).

Mutations in the plectin gene (*PLEC1*) are generally thought to cause epidermolysis bullosa simplex (EBS) associated with muscular dystrophy. The majority of these cases are characterized by generalized blistering and muscular dystrophy (McLean *et al.*, 1996; Smith *et al.*, 1996; Shimizu *et al.*, 1999). Muscle weakness is first observed during the latter part of the first decade of life. However, we and other groups have recently demonstrated that lethal EBS cases with pyloric atresia (EBS-PA) also result from mutations in *PLEC1* (Nakamura *et al.*, 2005; Pfendner and Uitto, 2005b). Seven cases of this new variant of EBS have been reported so far (Pfendner *et al.*, 2005a). These patients manifest with cutaneous blisters, aplasia cutis congenital (severe localized absence of skin), and pyloric atresia, which rapidly result in the patient's demise, often soon after birth. This study reports two cases with defective plectin expression that show EBS-PA and EBS with muscular dystrophy (EBS-MD). Furthermore, based on data mining from the *PLEC1* mutation database, we suggest the possible involvement of exon 31 in alternative splicing that may alleviate the phenotypic severity of epidermolysis bullosa cases caused by mutations in the plectin gene.

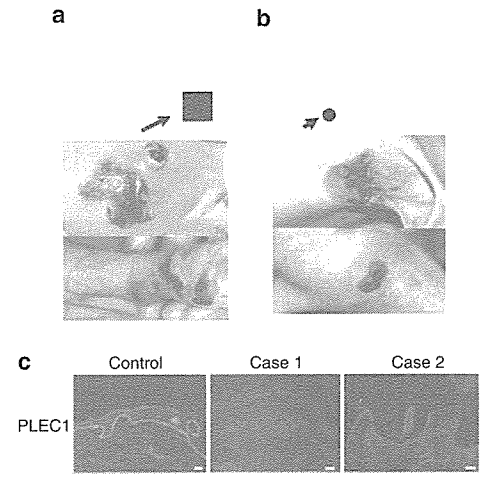

Figure 1. Family trees, clinical findings and plectin expression. (**a**) Case 1 was a 4-month-old boy who has exhibited skin fragility since birth. There was no family history of skin fragility. Blisters and erosions were scattered over his whole body and oral mucous membranes were also affected. Healing occurred without scarring and milia formation. He was diagnosed as suffering from pyloric atresia by routine abdominal X-ray. On the fourth day after birth, pyloroplasty was performed. He suffered from aspiration pneumonia and impairment of weight gain before the age of 6 months, but afterwards the volume of milk taken increased and blister formation steadily lessened. No muscular and neurological findings were observed. (**b**) Case 2 was a 49-year-old female with skin fragility from birth. Several blisters and erosions were found on her trunk and extremities. Slight scar formation was seen in some areas. Hypoplasty of her permanent dentition was seen and some nail thickening was observed. Her family tree showed a history of consanguinity. Although mild blister formation continued, muscle symptoms had never been found, until muscle weakness on the arms was first noted at the age of 19 years. Muscle weakness gradually progressed, but she was able to perform routine activities. However, she could not walk at the age of 38 years, owing to widespread muscular atrophy. She is now confined to a bed and breathing is assisted by a respirator. (**c**) Direct immunofluorescence analysis using mAb HD1-121 against plectin (a kind gift from Dr Owaribe K, Nogoya University) demonstrated that immunoreactivities were markedly attenuated in cases 1 and 2 compared with normal control. Bar = 50 μm

Case 1 was a 4-month-old boy with skin fragility from birth. There was no other family history of skin fragility (Figure 1a). Generalized blisters and erosions were found over his entire body. He was diagnosed as suffering from pyloric atresia by routine abdominal X-ray. Case 2 was a 49-year-old female with skin fragility from birth (Figure 1b). Family tree showed a history of consanguinity, although there was no other family history of skin fragility. She is now bedridden and

Abbreviations: EBS, epidermolysis bullosa simplex; EBS-MD, epidermolysis bullosa simplex associated with muscular dystrophy; EBS-PA, epidermolysis bullosa simplex associated with pyloric atresia; PTC, premature termination codon

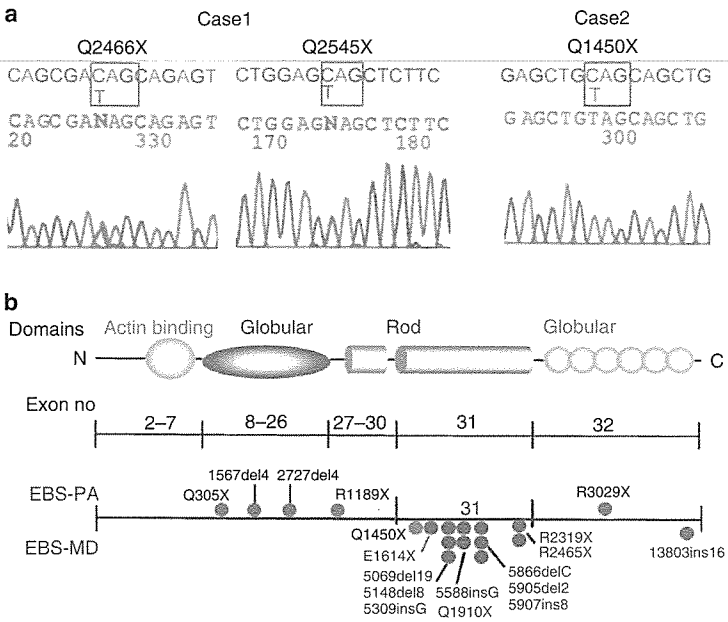

Figure 2. ***PLEC1* mutations and significance of exon 31** (**a**) Genomic DNA was obtained from both cases and the parents. The mutation detection strategy was performed after PCR amplification of all exons and intron-exon borders, followed by direct automated nucleotide sequencing. The genomic DNA nucleotides, the complementary DNA nucleotides and the amino acids of the protein were numbered based on the previous sequence information (GenBank accession no. AH003623) (McLean *et al.*, 1996). Case 1 demonstrated heterozygous nonsense mutations. The maternal nonsense mutation was a C → T transition at nucleotide c.7396 of complementary DNA in exon 31, resulting in the substitution of a glutamine (CAG) at position 2466 with a stop codon (TAG) (Q2466X). The other paternal nonsense mutation was also a C → T transition at nucleotide c.7633 of complementary DNA in exon 32, resulting in the substitution of a glutamine (CAG) at position 2545 with a stop codon (TAG) (Q2545X). Case 2 showed homozygous nonsense mutations, which was a C → T transition at nucleotide c.4348 of complementary DNA in exon 31, resulting in the substitution of a glutamine (CAG) at position 1450 with a stop codon (TAG) (Q1450X). (**b**) The plectin database shows many homozygous mutations and we plotted the position of only homozygous PTC mutations. Interestingly, homozygous PTC mutations associated with EBS-MD (blue circles) are located in exon 31 except for one mattation13803ins16 whereas those with EBS-PA (red circles) are in other parts of the gene except exon 31. Q1450X (green circle) is the present case. Amino-terminal actin binding domain, amino-terminal globular domain, rod domain and carboxyl-terminal globular domain are shown. Positions of exons are indicated by numbers (exon no).

requires a respirator owing to progressive muscular dystrophy. Some blisters and erosions were observed on her trunk and extremities.

An immunohistochemical study using mAbs to a range of basement membrane zone component proteins was performed. Immunoreactivity against plectin rod domain was markedly attenuated in cases 1 and 2 (Figure 1c). Immunostaining for other basement membrane zone proteins including bullous pemphigoid antigens 1 and 2, the $\alpha 6$ and $\beta 4$ integrins, laminin 5, and type VII collagens were normal (data not shown). Direct nucleotide sequencing of *PLEC1* demonstrated that case 1 harbored novel heterogeneous premature termination codon (PTC) mutations Q2466X in exon 31 and Q2545X in exon 32, whereas case 2 harbored a novel homozygous PTC mutation, Q1450X, in exon 31 (Figure 2a). Informed consent was obtained from all individual subjects in this study. The protocols were approved by the Ethical Committee at Hokkaido University Graduate School of Medicine. This study was conducted according to the Declaration of Helsinki Principles.

Cases 1 and 2 demonstrated extracutaneous involvement including PA and MD, respectively. We believe that the clinical features and course of case 2 were typical of EBS-MD. Although all seven previous cases of EBS-PA showed a severe, lethal clinical course (Pfendner *et al.*, 2005a), case 1 was much milder than those cases and even showed some clinical improvement over time, so this is the first case of EBS-PA with a relatively moderate phenotype.

The precise pathomechanism causing the clinical differences between EBS-MD and EBS-PA has not yet been elucidated (Nakamura *et al.*, 2005; Pfendner *et al.*, 2005a; Pfendner and Uitto, 2005b). The *PLEC1* mutation database has accumulated almost 40 *PLEC1* mutations from 22 cases of EBS-MD and seven cases of EBS-PA (Pfendner *et al.*, 2005a, McMillan *et al.*, 2007). We have carefully re-examined genotype–phenotype correlations in EBS-MD and EBS-PA. The plectin database contains many homozygous mutations and we plotted only homozygous PTC mutations in order to minimize the effect of the expression difference between the two *PLEC1* alleles. Interestingly, homozygous PTC mutations associated with EBS and MD are located in exon 31 except for one (13803ins16), whereas those with EBS with PA are located in parts of the gene other than exon 31 (Figure 2b). Thus, the plectin database suggested that EBS-MD and EBS-PA were associated with mutations in exon 31 and other than in exon 31, respectively.

Analysis of the murine plectin gene showed that alternative splicing resulted in more than 16 plectin variants and that tissue-specific expression of these variants was different (Fuchs *et al.*, 1999; Rezniczek *et al.*, 2003). This leads to the possibility that PLEC1 alternative splicing affects the severity of blistering and extracutaneous manifestation. Plectin comprises a central rod domain with a α-helical coiled-coil structure and large flanking amino-and carboxyl-terminal globular domains (Liu *et al.*, 1996; Wiche, 1998). Recently, one alternate splice messenger RNA transcript which lacks exon 31 encoding the central rod domain was identified in multiple rat tissues (Elliott *et al.*, 1997; Steinboeck and Kristufek (2005)). In fact, skin fragility in patients

with *PLEC1* mutations was less severe than that observed in plectin-deficient mice. As most of *PLEC1* mutations are located within the rod domain that was not present in the smaller splice variant, this variant might in part compensate for the loss of the canonical (full length) plectin expression in humans (Litjens *et al.*, 2006). To understand the expression of the rodless alternative spliced form in various human tissues and cells, we performed plectin domain-specific RT-PCR, which indicated that human cells also express the rodless isoform at various levels (data not shown).

A combination of our mutations and plectin expression results with the above mutation database, suggests that exon 31 alternate splicing may restore the *PLEC1* open-reading frame in EBS-MD patients with PTC mutations in exon 31, and partially rescue the phenotype. Therefore, we suggest that EBS-MD caused by mutations in exon 31 demonstrates a milder phenotype than EBS-PA caused by non-exon 31 *PLEC1* mutations. Furthermore, the relatively moderate phenotype of case 1 with non-lethal EBS-PA might result from one mutation associated with exon 31.

CONFLICT OF INTEREST

The authors state no conflict of interest.

ACKNOWLEDGMENTS

We thank Akari Nagasaki for her technical assistance. This work was supported in part by a Grant-in-Aid for Scientific Research from the Japanese Society for the Promotion of Science and by a Health and Labour Sciences Research Grant. We thank the patients and their family for their interest in our study. We thank the referring physicians for providing clinical information.

Daisuke Sawamura[1], Maki Goto[1], Kaori Sakai[1], Hideki Nakamura[1], James R. McMillan[1], Masashi Akiyama[1], Osamu Shirado[2], Noritaka Oyama[3], Masataka Satoh[3], Fumio Kaneko[3], Toshiaki Takahashi[4], Hidehiko Konno[4] and Hiroshi Shimizu[1]

[1]Department of Dermatology, Hokkaido University Graduate School of Medicine, Sapporo, Japan; [2]Division of Spine Surgery, Department of Orthopedic Surgery, Hokkaido University Graduate School of Medicine, Sapporo, Japan; [3]Department of Dermatology, Graduate School of Medicine, Fukushima Medical University, Fukushima, Japan and [4]Department of Neurology and Division of Clinical Research, Nishitaga National Hospital, Sendai, Japan
E-mail: smartdai@med.hokudai.ac.jp

REFERENCES

Elliott CE, Becker B, Oehler S, Castanon MJ, Hauptmann R, Wiche G (1997) Plectin transcript diversity: identification and tissue distribution of variants with distinct first coding exons and rodless isoforms. *Genomics* 42:115–25

Fine JD, Eady RA, Bauer EA, Briggaman RA, Bruckner-Tuderman L, Christiano A *et al.* (2000) Revised classification system for inherited epidermolysis bullosa: Report of the Second International Consensus Meeting on diagnosis and classification of epidermolysis bullosa. *J Am Acad Dermatol* 42:1051–66

Fuchs P, Zorer M, Rezniczek GA, Spazierer D, Oehler S, Castanon *et al.* (1999) Unusual 5′ transcript complexity of plectin isoforms: novel tissue-specific exons modulate actin binding activity. *Hum Mol Genet* 8:2461–72

Litjens SH, de Pereda JM, Sonnenberg A. (2006) Current insights into the formation and breakdown of hemidesmosomes. *Trends Cell Biol* 16:376–83

Liu CG, Maercker C, Castanon MJ, Hauptmann R, Wiche G (1996) Human plectin: organization of the gene, sequence analysis, and chromosome localization (8q24). *Proc Natl Acad Sci USA* 93:4278–83

McLean WH, Pulkkinen L, Smith FJ, Rugg EL, Lane EB, Bullric F *et al.* (1996) Loss of plectin causes epidermolysis bullosa with muscular dystrophy; cDNA cloning and genomic organization. *Genes Dev* 10:1724–35

McMillan JR, Akiyama M, Rouan F, Mellerio JE, Lane EB, Leigh IM *et al.* (2007) Plectin defects in epidermolysis bullosa simplex with muscular dystrophy. *Muscle Nerve* 35:24–35

Nakamura H, Sawamura D, Goto M, Nakamura H, McMillan JR, Park S *et al.* (2005) Epidermolysis bullosa simplex associated with pyloric atresia is a novel clinical subtype caused by mutations in the plectin gene (*PLEC1*). *J Mol Diagn* 7:28–35

Pulkkinen L, Uitto J (1999) Mutations analysis and molecular genetics of epidermolysis bullosa. *Matrix Biol* 18:29–42

Pfendner E, Rouan F, Uitto J (2005a) Progress in epidermolysis bullosa: the phenotypic spectrum of plectin mutations. *Exp Dermatol* 14:241–9

Pfendner E, Uitto J (2005b) Plectin gene mutations can cause epidermolysis bullosa with pyloric atresia. *J Invest Dermatol* 124:111–5

Rezniczek GA, Abrahamsberg C, Fuchs P, Spazierer D, Wiche G (2003) Plectin 5′-transcript diversity: short alternative sequences determine stability of gene products, initiation of translation and subcellular localization of isoforms. *Hum Mol Genet* 12:3181–94

Shimizu H, Takizawa Y, Pulkkinen L, Murata S, Kawai M, Hachisuka H *et al.* (1999) Epidermolysis bullosa simplex associated with muscular dystrophy phenotype–genotype correlation and review of the literature. *J Am Acad Deramtol* 41:950–6

Smith FJ, Eady RA, Leigh IM, McMillan JR, Rugg EL, Kelsell DP *et al.* (1996) Plectin deficiency results in muscular dystrophy with epidermolysis bullosa. *Nat Genet* 13:450–7

Steinboeck F, Kristufek D (2005) Identification of the cytolinker protein plectin in neuronal cellst – expression of a rodless isoform in neurons of the rat superior cervical ganglion. *Cell Mol Neurobiol* 25:1151–69

Wiche G (1998) Role of plectin in cytoskeleton organization and dynamics. *J Cell Sci* 111:2477–86

A Novel *GJB2* Mutation p.Asn54His in a Patient with Palmoplantar Keratoderma, Sensorineural Hearing Loss and Knuckle Pads

Journal of Investigative Dermatology advance online publication, 25 January 2007; doi:10.1038/sj.jid.5700711

TO THE EDITOR

Mutations in the *GJB2* gene encoding connexin26 are the major cause of autosomal-recessive or -dominant non-syndromic congenital sensorineural hearing loss (SNHL) (Kelsell *et al.*, 1997; Kenneson *et al.*, 2002; refer to the connexin-deafness homepage at http://davinci.crg.es/deafness/). In addition, connexin26 mutations have been identified in autosomal-dominant syndromic congenital SNHL with palmoplantar keratoderma (PPK) (Maestrini *et al.*, 1999; Richard *et al.*, 2002, 2004; Brown *et al.*, 2003; van Steensel *et al.*, 2004; Arita *et al.*, 2006). We have encountered a Japanese boy with PPK, knuckle pads and congenital SNHL and *GJB2* mutation analysis revealed a novel mutation p.Asn54His.

The patient was a 12-year-old Japanese boy with PPK, knuckle pads on the fingers and severe SNHL. He had a congenital onset of profound bilateral SNHL. At 1 year of age, he developed PPK and knuckle pads. There was no familial history of skin disorders or auditory dysfunction. At age 12, moderate PPK was seen. Knuckle pads were apparent on all his fingers (Figure 1a and b). Acneiform follicular keratotic papules were seen on his forehead and face, although these acneiform papules might just be acne. No mutilation (pseudoainhum) was seen on the fingers. Nails, hair, and teeth were normal and no leukonychia was observed. Ophthalmologic examination revealed no apparent abnormality.

The medical ethical committee at Hokkaido University approved all studies described below. The study was conducted according to the Declaration of Helsinki Principles. Participants or their legal guardian gave their written informed consent. The coding region of *GJB2* (Genbank accession no. NM 004004) was amplified from genomic DNA by PCR, as described previously (Richard *et al.*, 1998). Direct sequencing of the patient's PCR products revealed that the patient was a heterozygote for a novel missense mutation p.Asn54His (A to C substitution at nucleotide position 160: asparagine 54 (AAC) to histidine (CAC)) in *GJB2* (Figure 1d), which was not found in his mother. We were unable to obtain a DNA sample from his father. This mutation was not found in 100 normal unrelated Japanese alleles (50 normal unrelated Japanese individuals) by direct sequence analysis and was unlikely to be a polymorphism (data not shown). Direct sequencing of all the exons and exon/intron borders of *GJB2* failed to detect any other pathogenic mutation in the patient's DNA.

A skin biopsy obtained from the palmar lesion revealed orthohyperkeratosis and mild regular acanthosis. Electron microscopy of the upper epidermal keratinocytes showed normal morphology with normal keratin network and keratohyalin granules. Gap junctions existed in all living epidermal layers, and the morphology of gap junctions was normal, showing a typical pentalaminar structure, 20 nm in width (Figure 1e).

Immunofluorescent stainings with rabbit polyclonal anti-connexin26 antibody (the epitope is a portion of the cytoplasmic loop of connexin26) (ZYMED Laboratories, San Francisco, CA) showed strong connexin26 expression in the upper layers of the wide rete ridge in the patient's palmar epidermis (Figure 1f), compared with weak connexin26 expression in the normal palmar epidermis (Figure 1g). The antibody used in this study binds to both normal and mutated connexin26 peptides. Thus, it was not clear whether the overexpressed connexin26 in the patient's epidermis was normal and/or mutated. Connexin43 immunostainings with mouse monoclonal anti-connexin43 antibody (clone 4E6.2) (Chemicon International, Temecula, CA) revealed that the expression of connexin43 was almost completely membranous and appeared similar both in the patient's and normal control skin (data not shown).

Bart–Pumphrey syndrome is characterized by knuckle pads, PPK, SNHL, and leukonychia (Bart and Pumphrey, 1967). The present patient cannot be diagnosed with Bart–Pumphrey syndrome because of a lack of nail involvement. In two families which were reported as suffering from Bart–Pumphrey syndrome and harboring *GJB2* mutations, an affected patient in one family did not show any leukonychia and, in the other family, two affected family members showed leukonychia, but the other three failed to show any leukonychia (Alexandrino *et al.*, 2005; Leonard *et al.*, 2005). In this context, leukonychia is not an essential clinical feature in the patients with knuckle pad formation, PPK, and SNHL. It is questionable whether Bart–Pumphrey syndrome having leukonychia as an essential characteristic/diagnostic feature is a distinct clinical entity from the knuckle pads, PPK, and SNHL phenotype. Thus, in this study, we have adopted the clinical entity "knuckle pads, PPK, and SNHL", instead of Bart–Pumphrey syndrome.

Abbreviations: PPK, palmoplantar keratoderma; SNHL, sensorineural hearing loss

Most pathogenic *GJB2* mutations causing both SNHL and skin manifestations cluster in the first extracellular loop of the connexin26 peptide (Richard *et al.*, 1998, 2004; Maestrini *et al.*, 1999; Heathcote *et al.*, 2000; Uyguner *et al.*, 2002; Oshima *et al.*, 2003; Yotsumoto *et al.*, 2003; Montgomery *et al.*, 2004; Alexandrino *et al.*, 2005; Leonard *et al.*, 2005). This fact clearly suggests that this extracellular domain is important for the correct formation and/or function of gap junctions. Indeed, the evolutionary conserved, first extracellular loop domain was reported to play an essential role in the assembly of connexon hemichannels, connexon–connexon interactions, voltage gating, and channel permeability (Rubin *et al.*, 1992; White *et al.*, 1995; Oshima *et al.*, 2003).

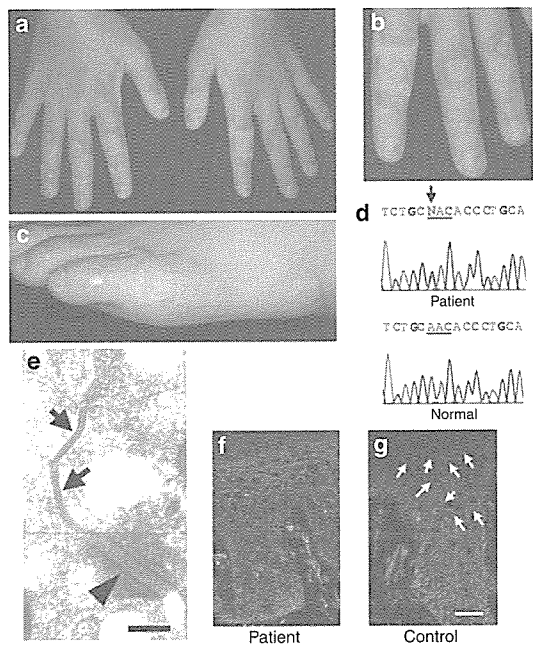

Figure 1. The patient's clinical features, *GJB2* mutation, gap junction ultrastructure and upregulated connexin26 expression. (**a–c**) The patient's clinical features at the age of 12. (**a**) Severe knuckle pads were seen over all the fingers. (**b**) The knuckle pads were sharply demarcated, hyperkeratotic plaques. (**b**) Nails were not involved. (**c**) Hyperkeratotic plaques resembling knuckle pads were seen in the toes and periphery of the foot. (**d**) Mutation in connexin26 gene (*GJB2*). A novel heterozygous A to C substitution at the codon 54 (c.160A>C) was detected in the patient's genomic DNA. This mutation leads to the amino-acid substitution, p.Asn54His. (**e**) A gap junction with normal, typical pentalaminar structure, 20 nm in width, was observed in the periphery of the keratinocyte in the lesional epidermis on the palm. Arrows, gap junction; arrowhead, desmosome. (**f**) Upregulated connexin26 expression was seen in the spinous layers of the patient's lesional skin in the palm. (**g**) In the normal control palmar skin, weak connexin26 immunostaining (green) was observed in the spinous layers (white arrows). Connexin26 immunostaining, green (FITC); nuclear staining, red (propidium iodide). (**e**) Bar = 100 nm and (**g**) 50 μm.

The causative *GJB2* missense mutations in the previously reported three families showing knuckle pads, PPK, and SNHL were a replacement of glycine 59 in two families (Alexandrino et al., 2005; Leonard *et al.*, 2005) and a replacement of asparagine 54 in the other family (Richard *et al.*, 2004), both in the evolutionary conserved first extracellular loop of connexin26. In the present case, the *GJB2* mutation similarly lay in the asparagine 54 residue. Asparagine was replaced by histidine in the present case and by lysine in the previously reported Bart–Pumphrey syndrome family (Richard *et al.*, 2004). Asparagine is an acidic amino acid and histidine and lysine are basic amino acids. Thus, the amino-acid exchange would probably result in an altered electron charge at the mutation site and may lead to defective voltage gating affecting the formation and function of gap junctions. In addition, histidine has a relatively large, aromatic side chain, and the amino-acid change may lead to a conforma-

Table 1. Mutations within the first extracellular domain of connexin26 and associated clinical features

Syndromes	KID syndrome		Knuckle pads, PPK, and SNHL			VWS	PPK and SNHL	
Causative mutations	p.Ala40Val	p.Asp50Asn/Tyr	p.Asn54Lys	p.Asn54His[1]	p.Gly59Arg/Ser	p.Asp66His	p.Gly59Ala	p.Arg75Trp/Gln
Knuckle pads	–	–	+	+	+	–	–	–
PPK	+	+	+	+	+	+	+	+
SNHL	+	+	+	+	+	+	+	+
Nail dystrophy (leukonychia)	+	+	±	–	–	–	–	–
Keratitis	+	+	–	–	–	–	–	–
Pseudoainhum	–	–	–	–	–	+	–	–

KID, keratitis–ichthyosis–deafness; PPK, palmoplantar keratosis; SNHL, sensorineural hearing loss; VWS, Vohwinkel syndrome; +, observed; –, not observed or not described; ±, observed in some case, but not in the others.
[1]Present case.

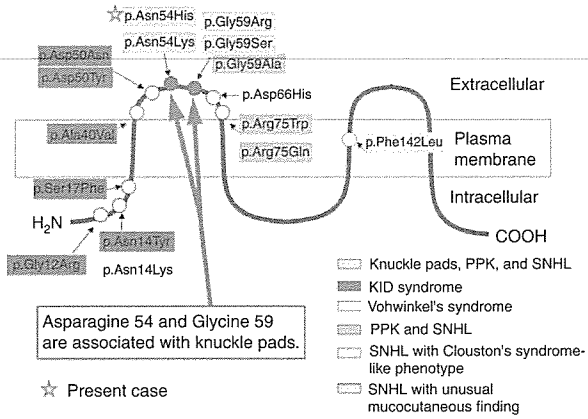

Figure 2. Connexin26 molecular structure, mutations and their associated skin syndromes. Connexin26 gene (*GJB2*) mutations associated with syndromic SNHL cluster in the N-terminal portion of connexin26, mainly in the first extracellular loop. Note all the mutations associated with knuckle pads affect asparagines 54 or glycine 59. Asterisk represents the present case.

tional change of the first extracellular domain in the present case. To determine the effect of this mutation on cell–cell gap junction function, functional studies by expressing the mutant allele in cultured cells are necessary.

Among the mutations located in the first extracellular loop of connexin26, differences in the site and nature of the mutations are thought to lead to the distinctive clinical phenotypes, as shown in Table 1 and Figure 2. These data including our case suggest that alterations of the amino-acid residues asparagines 54 and glycine 59 in the central portion of the first extracellular loop might be associated with the clinical knuckle pad feature, although we do not have any direct evidence to support that the mutations caused knuckle pads. Further accumulation of the similar cases should be needed to conclude this mutation lead to knuckle pads.

CONFLICT OF INTEREST

The authors state no conflict of interest.

ACKNOWLEDGMENTS

We thank the patient and his family for their generous cooperation and Ms Akari Nagasaki and Ms Satoko Ishikawa for their fine technical assistance on this project. This work was supported in part by Grant-in-Aid from the Ministry of Education, Science, Sports, and Culture of Japan to M. Akiyama (Kiban B 18390310).

Masashi Akiyama[1], Kaori Sakai[1], Ken Arita[1], Yukiko Nomura[1], Kei Ito[1], Kazuo Kodama[1], James R. McMillan[1], Kinuko Kobayashi[2], Daisuke Sawamura[1] and Hiroshi Shimizu[1]

[1]Department of Dermatology, Hokkaido University Graduate School of Medicine, Sapporo, Japan and [2]Kobayashi Skin Clinic, Sapporo, Japan
E-mail: akiyama@med.hokudai.ac.jp

REFERENCES

Alexandrino F, Sartorato EL, Marques-de-Faria AP, Steiner CE (2005) G59S mutation in the *GJB2* (connexin 26) gene in a patient with Bart–Pumphrey syndrome. *Am J Med Genet* 136A:282–4

Arita K, Akiyama M, Aizawa T, Umetsu Y, Segawa I, Goto M *et al.* (2006) A novel N14Y mutation in connexin26 in KID syndrome – analyses of altered gap junctional communication and molecular structure of N-terminus of mutated connexin26. *Am J Pathol* 169: 416–23

Bart RS, Pumphrey RE (1967) Knuckle pads, leukonychia and deafness – a dominant inherited syndrome. *New Engl J Med* 276:202–7

Brown CW, Levy ML, Flaitz CM, Reid BS, Manolidis S, Hebert AA *et al.* (2003) A novel GJB2 (connexin 26) mutation, F142L, in a patient with unusual mucocutaneous findings and deafness. *J Invest Dermatol* 121:1221–3

Heathcote K, Syrris P, Carter ND, Patton MA (2000) A connexin 26 mutation causes a syndrome of sensorineural hearing loss and palmoplantar hyperkeratosis (MIM 148350). *J Med Genet* 37:50–1

Kelsell DP, Dunlop J, Stevens HP, Lench NJ, Liang JN, Parry G *et al.* (1997) Connexin 26 mutations in hereditary non-syndromic sensorineural deafness. *Nature* 387:80–3

Kenneson A, Van Naarden Braun K, Boyle C (2002) GJB2 (connexin 26) variants and nonsyndromic sensorineural hearing loss: a HuGE review. *Genet Med* 4:258–74

Leonard NJ, Krol AL, Bleoo S, Somerville MJ (2005) Sensorineural hearing loss, striate palmoplantar hyperkeratosis, and knuckle pads in a patient with a novel connexin 26 (GJB2) mutation. *J Med Genet* 42:e2

Maestrini E, Korge BP, Ocana-Sierra J, Calzolari E, Cambiaghi S, Scudder PM *et al.* (1999) A missense mutation in connexin26, D66H, causes mutilating keratodermawith sensorineural deafness (Vohwinkel's syndrome) in three unrelated families. *Hum Mol Genet* 8:1237–43

Montgomery JR, White TW, Martin BL, Turner ML, Holland SM (2004) A novel connexin 26 gene mutation associated with features of the keratitis–ichthyosis–deafness syndrome and the follicular occlusion triad. *J Am Acad Dermatol* 51:377–82

Oshima A, Doi T, Mitsuoka K, Maeda S, Fujiyoshi Y (2003) Roles of M34, C64, and R75 in the assembly of human connexin 26: implication for key amino acid residues for channel formation and function. *J Biol Chem* 278:1807–16

Richard G, Brown N, Ishida-Yamamoto A, Krol A (2004) Expanding the phenotypic spectrum of Cx26 disorders: Bart–Pumphrey syndrome is caused by a novel missense mutation in GJB2. *J Invest Dermatol* 123: 856–63

Richard G, Rouan F, Willoughby CE, Brown N, Chung P, Ryynanen M *et al.* (2002) Missense mutations in GJB2 encoding connexin-26 cause the ectodermal dysplasia keratitis–ichthyosis–deafness syndrome. *Am J Hum Genet* 70:1341–8

Richard G, White TW, Smith LE, Bailey RA, Compton JG, Paul DL *et al.* (1998) Functional defects of Cx26 resulting from a heterozygous missense mutation in a family with dominant deaf-mutism and palmoplantar keratoderma. *Hum Genet* 103:393–9

Rubin JB, Verselis VK, Bennett MV, Bargiello TA (1992) Molecular analysis of voltage dependence of heterotypic gap junctions formed by connexins 26 and 32. *Biophys J* 62:183–93

Uyguner O, Tukel T, Baykal C, Eris H, Emiroglu M, Hafiz G *et al.* (2002) The novel R75Q mutation in the GJB2 gene causes autosomal dominant hearing loss and palmoplantar keratoderma in a Turkish family. *Clin Genet* 62:306–9

van Steensel MA, Steijlen PM, Bladergroen RS, Hoefsloot EH, Ravenswaaij-Arts CM, van Geel M (2004) A phenotype resembling the Clouston syndrome with deafness is associated with a novel missense GJB2 mutation. *J Invest Dermatol* 123:291–3

White TW, Paul DL, Goodenough DA, Bruzzone R (1995) Functional analysis of selective interactions among rodent connexins. *Mol Biol Cell* 6:459–70

Yotsumoto S, Hashiguchi T, Chen X, Ohtake N, Tomitaka A, Akamatsu H *et al.* (2003) Novel mutations in GJB2 encoding connexin-26 in Japanese patients with keratitis–ichthyosis–deafness syndrome. *Br J Dermatol* 148: 649–53

FEBS Letters 581 (2007) 535–540

Gelsolin segment 5 inhibits HIV-induced T-cell apoptosis via Vpr-binding to VDAC

Hongjiang Qiao*, James R. McMillan

Department of Dermatology, Hokkaido University Graduate School of Medicine, Kita-15, Nishi-7, Kita-Ku, Sapporo 060-0815, Japan
Creative Research Initiative, Faculty of Science, Hokkaido University, Kita-15, Nishi-7, Kita-Ku, Sapporo 060-0815, Japan

Received 25 October 2006; revised 19 December 2006; accepted 28 December 2006

Available online 17 January 2007

Edited by Richard Marais

Abstract **Viral protein R (Vpr) from the human immunodeficiency virus induces cell cycle arrest in proliferating cells, stimulates virus transcription, and regulates activation and apoptosis of infected T-lymphocytes. We report that Jurkat cells overexpressing full-length gelsolin show resistance to Vpr-induced T-cell apoptosis with abrogation of mitochondrial membrane potential loss and the release of cytochrome *c*. Co-immunoprecipitation assays in HEK293T cells demonstrated that overexpression of full-length or segment 5 (G5) but not G5-deleted gelsolin (ΔG5) bound to the voltage-dependent anion channel (VDAC), and that the G5 subunit can inhibit HIV-1-Vpr-binding to VDAC. We also confirmed that full-length gelsolin has the same effect in Jurkat cells. Clonogenic analysis showed that transfection of G5 but not ΔG5 cDNA protects Jurkat T cells from HIV-Vpr-Tet induced T-cell apoptosis and promoted cell survival, as did full-length gelsolin. These results suggest that the gelsolin G5 domain inhibits HIV-Vpr-induced T-cell apoptosis by blocking the interaction between Vpr and VDAC, and might be used as a protective treatment against HIV-Vpr-induced T-cell apoptosis.**

Keywords: Cytoskeletal protein; AIDS; Mitochondria; Cell death

1. Introduction

Multiple mechanisms have been proposed to explain the death and dysfunction of CD4+ T-cells after infection with the human immunodeficiency virus type 1 (HIV-1) [1]. There are various molecular HIV-1 components that play a role in the induction of apoptosis in T-lymphocytes [1]. Viral protein R (Vpr) plays an important role in regulating the nuclear transport of the HIV-1 pre-integration complex, and is required for virus replication in non-dividing cells [2,3]. Vpr also induces cell cycle arrest in proliferating cells, stimulates virus transcription, and regulates activation and apoptosis in infected cells [2,4,5]. These changes occur in the absence of other viral gene products, suggesting that Vpr mediates its proviral effects at least partially or perhaps solely, through modulation of the state of the target cell rather than directly by the virus [3]. Vpr from HIV-1 attaches to mitochondrial membranes and induces mitochondrial membrane permeabilization (MMP), which is a critical step in the regulation of apoptosis and is often accompanied by mitochondrial swelling and fragmentation [6,7].

Gelsolin, an actin-regulatory protein that modulates actin assembly and disassembly, is found as both an intrinsic cytoplasmic protein and secreted plasma protein [8,9]. In addition, gelsolin was identified as a substrate for caspase-3 by screening the translation products of small complementary DNA pools for sensitivity to cleavage by caspase-3 [10]. Expression of gelsolin cleavage product in multiple cell types caused the cells to detach, round up, and undergo nuclear fragmentation [10]. It was proposed that its association with actin drives the calcium-independent activation of the N-terminal three domains gelsolin G1–G3 during apoptosis [11]. Conversely, some reports have previously shown that cytoplasmic gelsolin is also present in the mitochondrial fraction of cells, and that full-length gelsolin can inhibit apoptosis of human Jurkat T-cells [12,13]. The overexpression of gelsolin inhibits the loss of mitochondrial membrane potential and cytochrome *c* release from mitochondria, resulting in a lack of activation of caspase −3, −8, and −9 in Jurkat cells treated with staurosporine, thapsigargin, and protoporphyrin IX [13]. This anti-apoptotic function of gelsolin was also observed in butyrate-induced apoptosis of colorectal cancer cells and the cholinergic toxin ethylcholine aziridinium-or amyloid-beta-induced apoptosis of neuronal cells [14–17], and segment G5 of human cytoplasmic gelsolin is sufficient for the function recorded in the latter case [17].

In this study, our efforts were directed towards investigating whether gelsolin can inhibit HIV-Vpr-induced cell death in Jurkat T cells, and to determine the specific gelsolin domain responsible for that function.

*Corresponding author. Fax: +81 11 706 7869.
E-mail address: qiao@igm.hokudai.ac.jp (H. Qiao).

Abbreviations: HIV-1, human immunodeficiency virus type 1; Vpr, viral protein R; VDAC, voltage-dependent anion channel; MMP, mitochondrial membrane permeabilization; IB, immunoblotting; Dox, doxycycline; PTPC, permeability transition pore complex; ANT, adenine nucleotide translocator; NMDA, *N*-methyl-D-aspartate; VDCC, voltage-dependent calcium channels; rtTA, reverse tetracycline-controlled transactivator; PI, propidium iodide; IP, immunoprecipitation

2. Results

2.1. Resistance of gelsolin-overexpressed Jurkat T-cells to HIV-Vpr-induced apoptosis

In an effort to determine whether overexpression of gelsolin in Jurkat T-cells affects HIV-Vpr-induced apoptosis, we used human cytoplasmic gelsolin-stably overexpressed in a Jurkat

0014-5793/$32.00
doi:10.1016/j.febslet.2006.12.057

T-cell clone JGF that was previously established [12]. To confirm continuous expression of gelsolin in JGF and Neo control clone JNF cells, immunoblotting (IB) analysis was performed. Gelsolin was not detected in JNF, while JGF displayed expression of gelsolin (90 KD) and was in keeping with previous results (Fig. 1A). The level of actin remained unchanged among all cell lines. Since we were not able to acquire HIV-Vpr stable transfectants using a constitutively expressing Vpr plasmid, we used an inducible expression system based on the tetracycline-responsive operon (Tet-on system) [18]. Jurkat Tet-on cell lines were created as described in Section 4 below that stably express FLAG-tagged HIV-Vpr by selection in medium containing hygromycin and zeocin. Several clones derived from cells transfected with HIV-Vpr were isolated, analyzed by IB analysis using anti-FLAG antibody to confirm the high expression of HIV-Vpr, and HIV-Vpr-overexpressed parental clone (JPV 5), JNF clones (JNFV 3, 4, 7) , and JGF clones (JGFV 2, 8, 9) were established. JP cells and all clone cells did not express HIV-Vpr under basic conditions (Fig. 1B). However, treatment with doxycycline (Dox) for 48 h resulted in a marked increase of recombinant Vpr protein expression without any detectable change in β-actin expression in parental cells and all clones. At different time points after Dox addition, JPV clone 5, JNFV clones (3, 4, 7) and JGF clones (2, 8, 9) were assayed for cell viability and apoptosis signs using Hoechst 33342 and PI staining. Hoechst 33342 staining showed HIV-Vpr-induced apoptosis accompanied by changes in nuclear morphology, such as nuclear condensation or fragmentation in control JNFV clones at 24, 48, 72 h after Dox treatment, while JGFV clones treated with Dox expressing HIV-Vpr failed to show any morphological nuclear changes (Fig. 2A). Cell viability analysis using Hoechst 33342 and PI revealed that all JGFV clones were clearly more resistant to apoptosis induced by Vpr compared to JPV clone 5 cells and all JNFV clones after 24 h (Dead cells: JGFV, 5% to JPV, 24%, JNFV, 23%), 48 h (Dead cells: JGFV, 9% to JPV, 46%, JNFV, 44%) and 72 h (Dead cells: JGFV, 12% to JPV, 55%, JNFV, 54%) (Fig. 2B) after initial Dox treatment. These data demonstrated that overexpression of gelsolin was associated with significant resistance to HIV-Vpr-induced apoptosis.

2.2. Inhibition of mitochondrial membrane potential loss and cytochrome c release stimulated with HIV-Vpr in gelsolin-overexpressed Jurkat T cells

Other report demonstrated that gelsolin can inhibit apoptosis induced by several apoptotic reagents by blocking signal transduction at the mitochondrial level upstream of the caspase cascade in human T lymphocytes [13]. To analyze the alteration in DeltaPsi(m) that follows HIV-Vpr apoptotic stimulation, we incubated cells after Dox treatment with the cationic dye Rhodamine 123 and then analyzed the cells using a flow-cytometer. JPV clone 5 and all JNF clones displayed loss of all mitochondrial potential, while JGFV clones demonstrated inhibitory activity (Fig. 3A). Another change observed in the mitochondria of apoptotic cells is the translocation of cytochrome *c* from within the innermost mitochondrial membrane to a cytosolic location. Immunoblot analysis of cytosolic fractions revealed that JPV clone 5 and all JNF clones showed cytochrome *c* release after Dox treatment, while there was almost no cytochrome *c* release from the JGF clones (Fig. 3B). Evaluation of all the data indicates that gelsolin

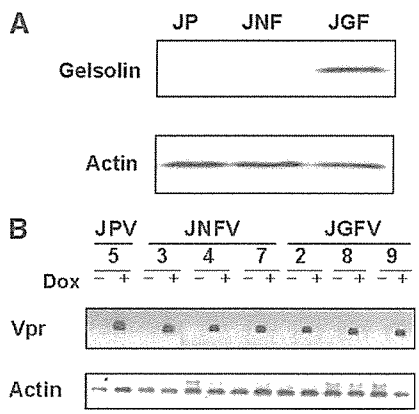

Fig. 1. Expression of gelsolin and HIV-Vpr in Jurkat cell lines by IB analysis. (A) Confirmation of stable expression of human full-length cytoplasmic gelsolin in Jurkat T cell line (JGF). JP, parental Jurkat cells; JNF, neo-transfected Jurkat clone. (B) Inducible expression of Flag-tagged HIV-Vpr in Jurkat Tet-on clones (JPV clone 5, JNFV clones 3, 4, 7, and JGFV clones 2, 8, 9) at 24 h in the absence or presence of 2 μg/ml Dox. The expression of actin was monitored to ensure equivalent loading and transfer.

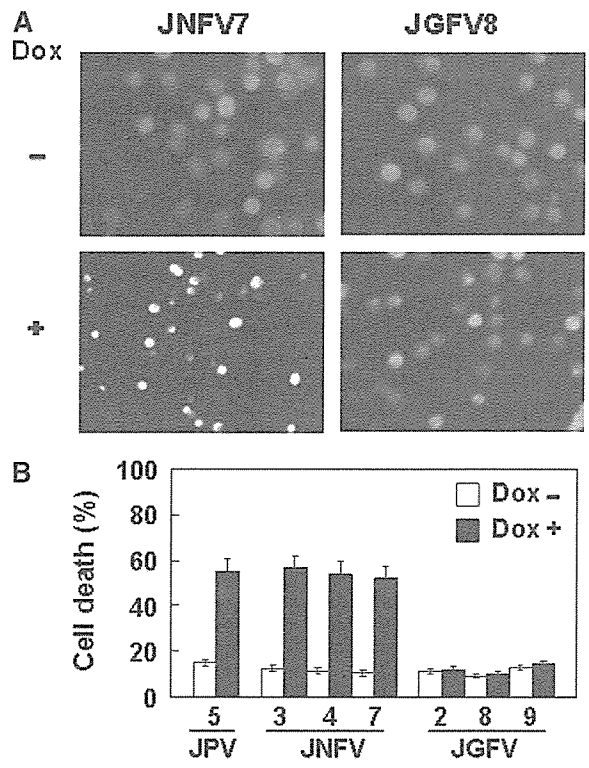

Fig. 2. Cell viability in HIV-Vpr expressed Jurkat cell lines. (A) Hoechst staining of HIV-Vpr expressed JNFV7 and JGFV8 cells at 72 h in the presence or absence of 2 μg/ml Dox. (B) Cell viability of JPV, JNFV, and JGFV cell lines at 72 h in the presence or absence of 2 μg/ml Dox was calculated as the percentage of apoptotic cells compared to total cells using Hoechst 33342 and PI. Three experiments were performed in duplicate, and values represent the mean + S.E. of dead cells.

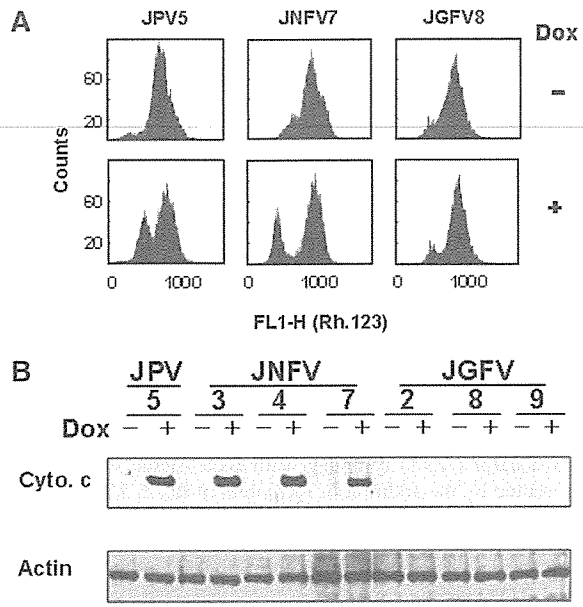

Fig. 3. MMP and cytochrome *c* release from mitochondria in HIV-Vpr expressed Jurkat cell lines. (A) MMP assessed by flow-cytometry with Rhodamine 123 of JPV5, JNFV7, and JGFV8 cells at 72 h in the presence or absence of 2 μg/ml Dox. (B) Cytochrome *c* release from mitochondria of JPV, JNFV, and JGFV cell lines at 72 h in the presence or absence of 2 μg/ml Dox.

can effectively inhibit HIV-Vpr-induced apoptosis at a point concomitant with, or upstream of, the mitochondrial events.

2.3. *Inhibition of HIV-Vpr binding to VDAC by full-length gelsolin and gelsolin segment 5 (G5)*

We have previously shown that segment 5 of gelsolin (G5) represents an important regulatory region in determining its inhibitory effect upon cell apoptosis [17]. Recent reports suggested that VDAC is a key molecule controlling apoptotic mitochondrial changes and the HIV-Vpr induces apoptosis via a direct effect on the mitochondrial permeability transition pore complex (PTPC) by binding VDAC [6]. To verify the interaction between full-length gelsolin, G5, and VDAC, co-immunoprecipitation experiments were performed. HEK293T cells were transiently transfected with an expression plasmid encoding Myc-tagged full-length gelsolin, G5, or G5-deleted gelsolin (ΔG5) together with expression plasmid encoding T7-tagged VDAC, and the cell lysates were immunoprecipitated with anti-Myc antibody. The resulting precipitates and a portion of the cell lysate were subjected to IB analysis with anti-T7 tag and anti-Myc antibodies. Results of IB analysis showed that VDAC coprecipitated with full-length gelsolin and the G5 domain, but not with ΔG5 transfectant, suggesting that gelsolin is physically associated with VDAC and that the G5 segment of gelsolin is necessary and by itself sufficient for this interaction (Fig. 4A).

The observed interaction allowed us to determine if gelsolin and HIV-Vpr compete for the binding of VDAC in cultured cells. HEK293T cells were transiently transfected with expression plasmids encoding Flag-tagged Vpr and T7-tagged VDAC, together with increasing amounts of expression plasmid for Myc-tagged G5 (Fig. 4B). Cell lysates were prepared from transfected cells, immunoprecipitated with anti-T7 tag antibody, and the resulting precipitates and a portion of cell lysate were subjected to IB analysis with anti-FLAG, anti-T7 tag and anti-Myc antibodies. The results of IB analysis showed that VDAC-bound-Vpr was reversibly reduced with the amount of G5 administered in a dose-dependent manner. The amounts of Vpr and VDAC expressed were almost constant. These results indicate that G5 blocks the interaction between HIV-Vpr and VDAC.

Therefore, we also examined the effect of full-length gelsolin on the physical interaction between Vpr and the VDAC in

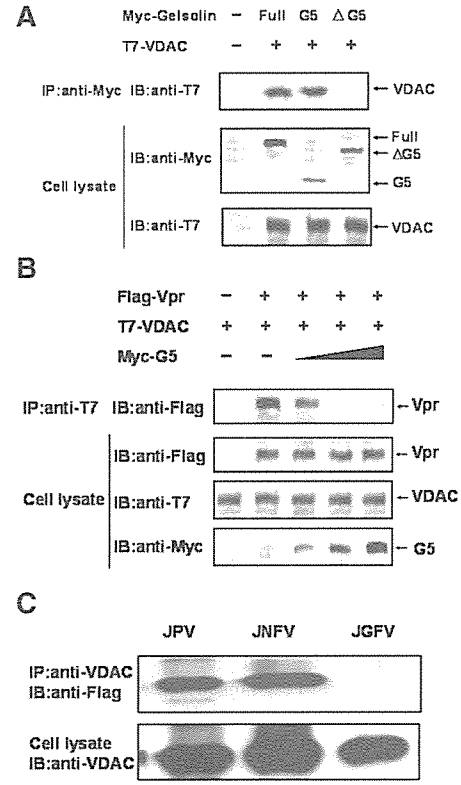

Fig. 4. Inhibition of VDAC-Vpr interaction by full-length gelsolin and the G5 segment of gelsolin. (A) HEK293T cells were transiently transfected with Myc-tagged full-length gelsolin (Full), G5 or ΔG5 (1 μg) together with T7-tagged VDAC (1 μg) as indicated. Cell lysates were subjected to immunoprecipitation (IP) with anti-Myc antibody, and the resulting precipitates were subjected to IB with anti-T7 tag antibody. A portion of the cell lysate was directly subjected to IB with anti-Myc, anti-T7 tag antibody in order to verify the expression level of gelsolin and VDAC proteins. (B) HEK293T cells were transfected with Flag-tagged HIV-Vpr and T7-tagged VDAC together with increasing amounts of Myc-G5 (0.5, 1, and 2 μg). Cell lysates were subjected to IP with anti-T7 tag antibody, and the resulting precipitates were subjected to IB with anti-FLAG antibody. A portion of the cell lysate was directly subjected to IB with anti-FLAG, anti-T7 tag, and anti-Myc antibodies to verify the expression level of Vpr, VDAC, and G5 proteins. (C) JPV, JNFV and JGFV cells were treated with Dox for 48 h. Cell lysates were subjected to IP with anti-VDAC antibody, and the resulting precipitates blotted with anti-Flag antibody. A portion of the cell lysate was directly subjected to IB with anti-VDAC in order to verify the VDAC protein expression level (internal control).

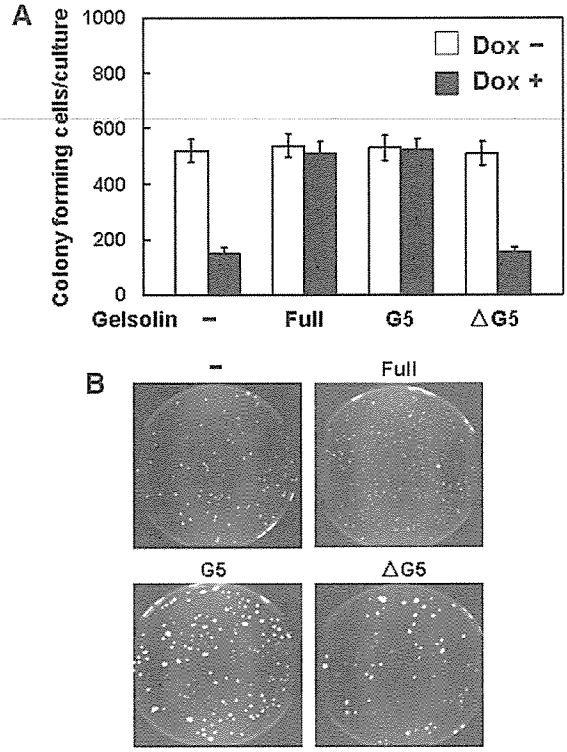

Fig. 5. G5 segment allows Dox-treated HIV-Vpr Tet-on Jurkat T cells to form colonies. (A) Cells were assayed for colony-forming ability 2 weeks after apoptotic induction by Dox treatment with the transfection of an empty plasmid (–), full-length gelsolin (Full), G5 or ΔG5 expression plasmids. Means and standard errors of two independent experiments each containing three replicates are shown. (B) Plates are illustrated below the corresponding Dox (+) columns of the histogram.

Jurkat cells, using an immunoprecipitation assay system (Fig. 4C). Cells were treated with Dox after 48 h, cell lysates were immunoprecipitated with anti-VDAC and the immunocomplexes probed with Flag tagged Vpr or gelsolin antibodies. These results showed that Vpr can interact with VDAC in JPV and JNFV cells, but this interaction cannot be detected in JGFV cells. These results demonstrate that Vpr is bound to VDAC in JPV clones and all JNFV clones, but this interaction was inhibited by full-length gelsolin overexpressing Jurkat cells after Dox treatment.

2.4. Protective function of G5 from HIV-Vpr-induced apoptosis in Jurkat T cells

In order to determine the protective function of full-length gelsolin and G5 from HIV-Vpr-induced apoptosis in the Jurkat cell line, we examined their effects by utilizing the most stringent criterion for cell survival: the ability to form a colony from only a single cell. Treatment of Dox in parental Jurkat HIV-Vpr Tet-on (JPV) clone 5 cell line with an empty control plasmid produced a substantial reduction in colonies that subsequently formed in soft agar (Fig. 5A and B). The transfection of expression plasmids with full-length gelsolin or G5, however, produced a 3.4-fold and 3.6-fold respective increase in the number of colony-forming cells surviving this treatment in the JPV clone 5 cells, while that of an empty or ΔG5 plasmids showed no such increase (Fig. 5A and B). These results indicate that the G5 domain and not ΔG5 has a protective function against HIV-Vpr-induced apoptosis in Jurkat T cells, similar to full-length gelsolin.

3. Discussion

HIV-Vpr causes a rapid dissipation of mitochondrial membrane potential, as well as a mitochondrial release of apoptogenic proteins such as cytochrome *c* or apoptosis inducing factor [6]. The effects of both mitochondrial and cytotoxic Vpr are prevented by Bcl-2, an inhibitor of the permeability transition pore complex (PTPC) [19]. Vpr favors the permeabilization of artificial membranes containing purified PTPC or defined PTPC components such as the adenine nucleotide translocator (ANT) combined with Bax. Again, this effect is prevented by the addition of recombinant Bcl-2. The Vpr carboxyl terminus binds purified ANT, as well as a molecular complex containing ANT and VDAC, another PTPC component. Vpr induces apoptosis via a direct effect on the mitochondrial PTPC [6,19].

Koya et al. previously reported that human cytoplasmic gelsolin is localized not only in the cytosol, but also in the mitochondrial fraction of cells, and that it inhibits the loss of DeltaPsi(m) and cytochrome *c* release from mitochondria in Jurkat cells treated with staurosporine, thapsigargin and protoporphyrin IX [13]. Furthermore, overexpression of gelsolin inhibits the loss of DeltaPsi(m) and cytochrome *c* release from mitochondria and inhibits activation of caspase −3, −8, and −9 in Jurkat cells treated with staurosporine, thapsigargin, and protoporphyrin IX. These effects were corroborated in vitro using recombinant gelsolin protein on isolated rat mitochondria stimulated with calcium, atractyloside, or Bax [13]. The carboxyl-terminal half of gelsolin may also prevent apoptotic mitochondrial changes such as DeltaPsi(m) loss and cytochrome *c* release in isolated mitochondria and inhibit the activity of VDAC on liposomes [20]. Segment 5 of human cytoplasmic gelsolin is the region responsible for inhibition of Amyloid beta-induced cytotoxicity in PC12 rat neuronal cells, in addition to full-length gelsolin [17]. Primary hippocampal neurons cultured from mice lacking gelsolin showed enhanced calcium influx after exposure to glutamate [15]. Whole-cell patch-clamp analyses showed that currents through *N*-methyl-D-aspartate (NMDA) receptors and voltage-dependent calcium channels (VDCC) were enhanced in hippocampal neurons lacking gelsolin. These results suggest roles for gelsolin in events that involve activation of NMDA receptors and VDCC [15]. In this report, we have uncovered another function of gelsolin associated with the ion channel by demonstrating binding to VDAC in mitochondria.

Here we report that gelsolin inhibits HIV-Vpr-induced apoptosis accompanied by the loss of DeltaPsi(m) and cytochrome *c* release from mitochondria in Jurkat T cells. We took advantage of the high transfection efficiency of HEK293T cells to study interactions between VDAC and gelsolin, and demonstrated binding between full-length gelsolin and the G5 segment, but not between other segments and VDAC. Moreover, we demonstrated in HEK293T cells that gelsolin segment 5 shows overlapping, competitive binding of VDAC with HIV-Vpr. These results suggest that gelsolin G5 domain inhibits

HIV-Vpr-induced T-cell apoptosis by blocking binding between Vpr and VDAC. In addition, similar results were obtained in Jurkat cells using full-length gelsolin.

There are reports showing that the presence of antioxidants, such as *N*-acetyl-cysteine, nicotinamide or L-acetyl-carnitine, were able to rescue most of the peripheral blood lymphocytes of subjects with acute HIV syndrome from apoptosis through a protective effect on mitochondria [21]. Additionally, IL-2 and IL-4 produced by peripheral blood mononuclear cells during highly active retroviral therapy provided anti-apoptotic signals that may contribute to an increased survival of T-cells and may thus play a part in long-term immune reconstitution [22]. In this report, we have demonstrated significant protection produced by the G5 gelsolin subunit, but not with other gelsolin domains, from HIV-Vpr-induced apoptotic induction of Jurkat T cells grow on soft agar. These findings suggest a rationale for the use of gelsolin segment 5 protein treatment, in addition to antiviral drugs, in primary HIV infection.

4. Materials and methods

4.1. Plasmid construction

To construct a mammalian expression plasmid with Myc-tagged human cytoplasmic gelsolin (pCI-neo-6xMyc-Gelsolin), the coding sequence was amplified by PCR using LKCG (a kind gift from D. Kwiatkowski of Harvard Medical School) as a template. The resulting PCR products were subcloned into the *EcoRI–SalI* site of the pCI-neo-6xMyc mammalian expression plasmid [23]. Two gelsolin mutants, G5 that encodes segment 5 of human gelsolin (amino acids 516–618) and ΔG5 that lacks the region encoding segment 5, were generated using a PCR-based method and the resulting PCR products were subcloned into pCI-neo-6xMyc, and pCI-neo-6xMyc-G5 and pCI-neo-6xMyc-ΔG5 were prepared, respectively. Human VDAC1 cDNA was obtained by RT-PCR using forward primer (5′-TATGAATTCATGTGTAACACACCAACG-3′) and reverse primer (5′-TATCTCGAGCCTCAAACCACATTAAGC-3′) [24], and the resulting PCR product was subcloned into the *EcoRI–SalI* site of pCI-neo-3xT7 as described previously [23], and pCI-neo-3XT7-VDAC was constructed. Vpr sequence derived from the plasmid vector pME18Neo-F(lag)Vpr containing HIV-1-Vpr [5] (a generous gift from Dr. Aida, Retrovirus Research Unit, RIKEN, Wako, Saitama, Japan) and the Flag tag-Vpr was subcloned into plasmid vector pTRE2-Hyg (Clontech) to generate the pTRE2-Hyg-Vpr plasmid.

4.2. Cell culture and establishment of stable cell lines

A lymphoblastoid T-cell line Jurkat (parental Jurkat: JP), and its stable clones transfected with human cytoplasmic gelsolin plasmid LKCG (JGF clone 5) or with the control plasmid LK444 (a kind gift from P. Gunning) (JNF clone 2), were maintained in RPMI 1640 medium containing 10% fetal calf serum (FCS) (Gibco BRL, Gaithersburg, MD) as described previously [12]. HEK293T cells was maintained in Dulbecco's modified Eagle's medium (DMEM) containing 10% FCS. All cells were cultured at 37 °C in a 5% CO2 humidified atmosphere.

The Tet-on system (Clontech, Mountain View, CA) was used to obtain stable cell lines that express HIV-1-Vpr. JP, JNF and JGF (1×10^6) were transfected with 2 μg of regulator plasmid pTracer-CMV2-Tet-on containing reverse tetracycline-controlled transactivator (rtTA), which interacts with the inducible promoter in the presence of tetracycline or analogues as Dox and activates transcription, and 12 μg/ml of SuperFect transfection reagent (Qiagen, Tokyo) according to the manufacturer's instructions. Each transfectant was selected in the presence of 0.8 mg/ml zeocin (Invitrogen, Carlsbad, CA). To select clones with high expression of rtTA, total RNA was isolated from JP-Tet-on JNF-Tet-on and JGF-Tet-on cell lines with extraction reagent (TRIzol, Invitrogen). The RT-PCR was performed with 1 μg of RNA from each sample, with reverse transcriptase (Superscript II; Gibco BRL, Carlsbad, CA) and random primer. The reverse transcript was incubated with Taq-polymerase and primers rtTA forward (5′-GAGGTCGGAATCGAAGGTTT-3′), which matches the coding strand of rtTA at positions 55–74, and rtTA reverse (5′-TCGTAATAATGGCGGCATAC-3′), which matches the reverse strand of rtTA at positions 513–522, as described previously [24], for 35 cycles (denaturing: 30 s 95 °C; annealing: 30 s 55 °C; elongation: 90 s 72 °C), followed by a 7 min 72 °C extension. Electrophoresis of PCR-products was performed on a 1% agarose gel containing ethidium bromide. JP-Tet-on JNF-Tet-on and JGF-Tet-on cell lines that expressed higher rtTA were selected. Next, the selected Tet-on cell lines, JP-Tet-on JNF-Tet-on and JGF-Tet-on, were transfected with pTRE2-Hyg-Vpr and each transfectant (JPV clone 5; JNFV clones 3, 4, 7; JGFV clones 2, 8, 9) was further selected in the presence of 400 μg/ml Hygromycin (Wako, Osaka, Japan). To investigate clones with high expression of HIV-Vpr, each Tet-on cell line was treated with 2 μg/ml of Dox and the expression of HIV-Vpr confirmed by IB.

4.3. Immunoblotting analysis

Total cells were extracted in SDS sample buffer (40 mM Tris–HCl, pH 7.4, 5% 2ME, 2% SDS, 0.05% bromphenol blue). Cell lysates were analyzed by SDS–polyacrylamide gel electrophoresis and IB as described previously [13,22] using monoclonal anti-human gelsolin (GS-2C4, Sigma), monoclonal anti-cytochrome *c* (Pharmingen, Mississauga, ON, Canada), anti-Myc monoclonal antibody (Clontech), anti-T7 tag monoclonal antibody (Novagen, San Diego, CA), monoclonal anti-FLAG (M2) antibody (Sigma), monoclonal anti-VDAC (Sigma) and anti-β-actin monoclonal antibody (Chemicon, Temecula, CA). The bound primary antibodies were incubated with peroxidase-conjugated anti-mouse IgG+M (Jackson ImmunoResearch Lab., West Grove, PA) and detected by ECL Western blotting detection reagents (Amersham Biosciences). Band images were detected by a LAS 1000 mini system (Fuji Film, Kanagawa, Japan).

4.4. Assays for cell viability and mitochondrial functions

Cell viability and apoptotic cell death were assessed using Hoechst 33342 (Sigma, St. Louis, MO) and propidium iodide (PI) staining, MMP assayed by the addition of Rhodamine 123 to the culture medium, and cytochrome *c* release from mitochondria into the cytosol of Jurkat cells evaluated by SDS–polyacrylamide gel electrophoresis followed by IB of the cytosolic fraction, as previously described [13]. For cell viability and mitochondrial functions, JPV, JNFV, and JGFV cell lines were examined at 24, 48 or 72 h and 72 h in the presence or absence of 2 μg/ml Dox, respectively.

4.5. Co-immunoprecipitation analysis

HEK293T cells were transiently transfected with expression plasmid as indicated. Forty-eight hours after transfection, the cells were washed with ice-cold Tris-buffered saline (TBS) and harvested. The cells were then lyzed with immunoprecipitation (IP) buffer containing 50 mm Tris–HCl (pH 7.5), 150 mm NaCl, 0.5% Triton X-100, 10% glycerol, 0.1 mM PMSF, 10 μg/ml aprotinin, 1 μg/ml chymostatin, 1 μg/ml leupeptin, and 1 μg/ml pepstatin. The lysates were incubated on ice for 30 min, and the cell debris was removed by centrifugation at 13000*g* for 20 min. The resulting supernatants were pretreated with 20 μl Protein G-Sepharose beads (Roche,Tokyo, Japan) at 4 °C for 1 h and was then incubated with 2 μg anti-T7 tag or anti-Myc monoclonal antibody and 20 μl Protein G-Sepharose beads at 4 °C for 2 h. The immunocomplex that was produced was washed five times with IP buffer. SDS-sample buffer was added to the beads, and the samples were boiled. The immunoprecipitates and the cell lysates were subjected to IB analysis. For JPFV, JNFV and JGFV cell lines, 48 h after treatment with Dox, the cell lysates were then incubated with 2 μg anti-VDAC monoclonal antibody under the same conditions as previously mentioned.

4.6. Clonogenic assay

Clonogenic analysis was performed as described previously [25]. Using electroporation, 1×10^7 JPV clone 5 cells were transfected with expression plasmids: pCI-neo-6xMyc, pCI-neo-6xMyc-Gelsolin, pCI-neo-6xMyc-G5 or pCI-neo-6xMyc-ΔG5. Forty-eight hours after transfection, both 2 μg/ml Dox and 1 mg/ml neomycin were added to the medium. All cells harvested from each plate were suspended in 5 ml of 0.5% agarose containing 20% FCS medium and then plated on the top of 5 ml of 1% semi-solidified agarose (Nacalai Tesque Inc. Kyoto. Japan) with the same medium in 10 cm plates. For each

vector control, full-length gelsolin, G5 and ΔG5 clones, triplicate plates were used. The plates were incubated for 2 weeks at 37 °C in the presence of 5% CO2 in an incubator. They were then stained with 0.5 ml of 0.005% Crystal Violet for more than 1 h. Colonies grown on agarose were counted using a microscope.

4.7. Statistical analysis

The data shown represent mean values of at least three different experiments, expressed as mean ± S.E. Student's *t* test was used to compare the data, and a *P* value of less than 0.05 was considered statistically significant.

Acknowledgments: This work was supported by a grant-in-aid from the Health and Labor Sciences Research Grant (research into Human Genome, Tissue Engineering) H17-Saisei-12 (J.R.M.). We also thank Drs. N. Kuzumaki and H. Shimizu for helpful discussion.

References

[1] Roshal, M., Zhu, Y. and Planelles, V. (2001) Apoptosis in AIDS. Apoptosis 6, 103–116.
[2] Bukrinsky, M. and Adzhubei, A. (1999) Viral protein R of HIV-1. Reviews in Medical Virology 9, 39–49.
[3] Ayyavoo, V., Mahalingam, S., Rafaeli, Y., Kudchodkar, S., Chang, D., Nagashunmugam, T., Williams, W.V. and Weiner, D.B. (1997) HIV-1 viral protein R (Vpr) regulates viral replication and cellular proliferation in T cells and monocytoid cells in vitro. Journal of Leukocyte Biology 62, 93–99.
[4] Emerman, M. (1996) HIV-1, Vpr and the cell cycle. Current Biology 6, 1096–1103.
[5] Nishizawa, M., Kamata, M., Mojin, T., Nakai, Y. and Aida, Y. (2000) Induction of apoptosis by the Vpr protein of human immunodeficiency virus type 1 occurs independently of G(2) arrest of the cell cycle. Virology 276, 16–26.
[6] Jacotot, E., Ravagnan, L., Loeffler, M., Ferri, K.F., Vieira, H.L., Zamzami, N., Costantini, P., Druillennec, S., Hoebeke, J., Briand, J.P., Irinopoulou, T., Daugas, E., Susin, S.A., Cointe, D., Xie, Z.H., Reed, J.C., Roques, B.P. and Kroemer, G. (2000) The HIV-1 viral protein R induces apoptosis via a direct effect on the mitochondrial permeability transition pore. J. Exp. Med. 191, 33–46.
[7] Basanez, G. and Zimmerberg, J. (2001) HIV and apoptosis death and the mitochondrion. J. Exp. Med. 193, F11–F14.
[8] Kwiatkowski, D.J., Stossel, T.P., Orkin, S.H., Mole, J.E., Colten, H.R. and Yin, H.L. (1986) Plasma and cytoplasmic gelsolins are encoded by a single gene and contain a duplicated actin-binding domain. Nature 323, 455–458.
[9] Sun, H.Q., Yamamoto, M., Mejillano, M. and Yin, H.L. (1999) Gelsolin, a multifunctional actin regulatory protein. J. Biol. Chem. 274, 33179–33182.
[10] Kothakota, S., Azuma, T., Reinhard, C., Klippel, A., Tang, J., Chu, K., McGarry, T.J., Kirschner, M.W., Koths, K., Kwiatkowski, D.J. and Williams, L.T. (1997) Caspase-3-generated fragment of gelsolin: effector of morphological change in apoptosis. Science 278, 294–298.
[11] Burtnick, L.D., Urosev, D., Irobi, E., Narayan, K. and Robinson, R.C. (2004) Structure of the N-terminal half of gelsolin bound to actin: roles in severing, apoptosis and FAF. EMBO J. 23, 2713–2722.
[12] Ohtsu, M., Sakai, N., Fujita, H., Kashiwagi, M., Gasa, S., Shimizu, S., Eguchi, Y., Tsujimoto, Y., Sakiyama, Y., Kobayashi, K. and Kuzumaki, N. (1997) Inhibition of apoptosis by the actin-regulatory protein gelsolin. EMBO J. 16, 4650–4656.
[13] Koya, R.C., Fujita, H., Shimizu, S., Ohtsu, M., Takimoto, T., Tsujimoto, Y. and Kuzumaki, N. (2000) Gelsolin inhibits apoptosis by blocking mitochondrial membrane potential loss and cytochrome *c* release. J. Biol. Chem. 275, 15343–15349.
[14] Klampfer, L., Huang, J., Sasazuki, T., Shirasawa, S. and Augenlicht, L. (2004) Oncogenic Ras promotes butyrate-induced apoptosis through inhibition of gelsolin expression. J. Biol. Chem. 279, 36680–36688, (Journal Article).
[15] Furukawa, K., Fu, W., Li, Y., Witke, W., Kwiatkowski, D.J. and Mattson, M.P. (1997) The Actin-severing protein gelsolin modulates calcium channel and NMDA receptor activities and vulnerability to excitotoxicity in hippocampal neurons. J. Neurosci. 17, 8178–8186.
[16] Harms, C., Bosel, J., Lautenschlager, M., Harms, U., Braun, J.S., Hortnagl, H., Dirnagl, U., Kwiatkowski, D.J., Fink, K. and Endres, M. (2004) Neuronal gelsolin prevents apoptosis by enhancing actin depolymerization. Mol. Cell. Neurosci. 25, 69–82.
[17] Qiao, H., Koya, R.C., Nakagawa, K., Tanaka, H., Fujita, H., Takimoto, M. and Kuzumaki, N. (2005) Inhibition of Alzheimer's amyloid-β peptide-induced reduction of mitochondrial membrane potential and neurotoxicity by gelsolin. Neurobiology of Aging 26, 849–855.
[18] Orth, P., Schnappinger, D., Hillen, W., Saenger, W. and Hinrichs, W. (2000) Structural basis of gene regulation by the tetracycline inducible Tet repressor-operator system. Nat. Struct. Biol. 7, 215–219.
[19] Jacotot, E., Ferri, K.F., El Hamel, C., Brenner, C., Druillennec, S., Hoebeke, J., Rustin, P., Metivier, D., Lenoir, C., Geuskens, M., Vieira, H.L., Loeffler, M., Belzacq, A.S., Briand, J.P., Zamzami, N., Edelman, L., Xie, Z.H., Reed, J.C., Roques, B.P. and Kroemer, G. (2001) Control of mitochondrial membrane permeabilization by adenine nucleotide translocator interacting with HIV-1 viral protein R and Bcl-2. J. Exp. Med. 193, 509–519.
[20] Kusano, H., Shimizu, S., Koya, R.C., Fujita, H., Kamada, S., Kuzumaki, N. and Tsujimoto, Y. (2000) Human gelsolin prevents apoptosis by inhibiting apoptotic mitochondrial changes via closing VDAC. Oncogene 19, 4807–4814.
[21] Andrea, C., Cristina, M., Nicola, M., Vanni, B., Anna, S., Bruno, D.R. and Claudio, F. (1997) Mitochondria alterations and dramatic tendency to undergo apoptosis in peripheral blood lymphocytes during acute HIV syndrome. AIDS 11, 19–26.
[22] Ensoli, F., Fiorelli, V., De Cristofaro, M., Collacchi, B., Santini Muratori, D., Alario, C., Sacco, G., Iebba, F. and Aiuti, F. (2002) Endogenous cytokine production protects T cells from spontaneous apoptosis during highly active antiretroviral therapy. HIV Medicine 3, 105–117.
[23] Nakagawa, K. and Kuzumaki, N. (2005) Transcriptional activity of megakaryoblastic leukemia 1 (MKL1) is repressed by SUMO modification. Genes to Cells 10, 835–850.
[24] Mao, M., Fu, G., Wu, J.S., Zhang, Q.H., Zhou, J., Kan, L.X., Huang, Q.H., He, K.L., Gu, B.W., Han, Z.G., Shen, Y., Gu, J., Yu, Y.P., Xu, S.H., Wang, Y., Chen, S.J. and Chen, Z. (1998) Identification of genes expressed in human CD34(+) hematopoietic stem/progenitor cells by expressed sequence tags and efficient full-length cDNA cloning. Proc. Natl. Acad. Sci. USA 95, 8175–8180.
[25] Longthorne, V.L. and Williams, G.T. (1997) Caspase activity is required for commitment to Fas-mediated apoptosis. EMBO J. 16, 3805–3812.